

RS-MoE: Mixture of Experts for Remote Sensing Image Captioning and Visual Question Answering

Hui Lin[†], Danfeng Hong[†], *Senior Member, IEEE*, Shuhang Ge[†], Chuyao Luo, Kai Jiang, Hao Jin, and Congcong Wen *Member, IEEE*

Abstract—Remote Sensing Image Captioning (RSIC) presents unique challenges and plays a critical role in applications such as environmental monitoring, urban planning, and disaster management. Traditional RSIC methods often struggle to produce rich and diverse descriptions. Recently, with significant advancements in Vision-Language Models (VLMs), efforts have emerged to integrate these models into the remote sensing domain and to introduce richly descriptive datasets specifically designed to enhance VLM training. However, most current RSIC models generally apply only fine-tuning to these datasets without developing models tailored to the unique characteristics of remote sensing imagery. This paper proposes RS-MoE, a first Mixture of Expert based VLM specifically customized for remote sensing domain. Unlike traditional MoE models, the core of RS-MoE is the MoE Block, which incorporates a novel Instruction Router and multiple lightweight Large Language Models (LLMs) as expert models. The Instruction Router is designed to generate specific prompts tailored for each corresponding LLM, guiding them to focus on distinct aspects of the RSIC task. This design not only allows each expert LLM to concentrate on a specific subset of the task, thereby enhancing the specificity and accuracy of the generated captions, but also improves the scalability of the model by facilitating parallel processing of sub-tasks. Additionally, we present a two-stage training strategy for tuning our RS-MoE model to prevent performance degradation due to sparsity. We fine-tuned our model on the RSICap dataset using our proposed training strategy. Experimental results on the RSICap dataset, along with evaluations on other traditional datasets where no additional fine-tuning was applied, demonstrate that our model achieves state-of-the-art performance in generating precise and contextually relevant captions. Notably, our RS-MoE-1B variant achieves performance comparable to 13B VLMs, demonstrating the efficiency of our model design. Moreover, our model demonstrates promising generalization capabilities by consistently achieving state-of-the-art performance on the Remote Sensing Visual Question Answering (RSVQA) task.

Index Terms—Remote Sensing, Vision Language Model (VLM), Multi-modal Large Language Model (MLLM), Mixture of Experts (MoE)

This work was supported in part by the National Key Research and Development Program of China (2021YFC3300500) and Beijing Nova Program (2024124). (Hui Lin, Danfeng Hong, and Shuhang Ge contributed equally to this work). (*Corresponding author: Congcong Wen*).

Hui Lin, Kai Jiang, and Hao Jin are with China Academy of Electronics and Information Technology, Beijing 100846, China. (e-mail: linhui@whu.edu.cn, kaijiang@mail.ustc.edu.cn, and jinhao1@cetc.com.cn)

D. Hong is with the Aerospace Information Research Institute, Chinese Academy of Sciences, 100094 Beijing, China, and also with the School of Electronic, Electrical and Communication Engineering, University of Chinese Academy of Sciences, Beijing 100049, China. (e-mail: hongdf@aircas.ac.cn).

Chuyao Luo is with the Department of Computer Science, Harbin Institute of Technology, Shenzhen 518055, China. (e-mail: luochuyao.dalian@gmail.com).

Shuhang Ge and Congcong Wen are with the Department of Electrical and Computer Engineering, New York University Abu Dhabi, Abu Dhabi, UAE. (e-mail: sg7484@nyu.edu and wencc@nyu.edu).

I. INTRODUCTION

Image captioning integrates computer vision and natural language processing to automatically generate descriptive text for images, effectively bridging the information gap between visual and linguistic domains. Unlike captioning of common natural images, remote sensing image captioning (RSIC) poses greater challenges due to the inherent characteristics of remote sensing images, which cover larger geographic areas and more diverse geographical objects. Consequently, RSIC tasks demand not only the description of geographic object information but also a comprehensive understanding of the relationships and interactions among various geographic objects.

Early studies of RSIC focused on traditional methodologies, including template-based [1] and retrieval-based methods [2], [3]. However, these methods cannot generate rich and varied descriptive sentences. Recent studies [4], [5], [6], [7] commonly adopt the encoder-decoder architecture, which divides the RSIC task into an image encoding phase that extracts semantic features from the input image, and a sequence modeling phase that uses the extracted features to generate text and sentences. Depending on the specific models employed, encoder-decoder approaches can be further categorized into CNN-based encoders with RNN/LSTM decoders, and CNN-based encoders with Transformer decoders. Although these methods have achieved satisfying performance on the RSIC task, they typically generate only one or two simple sentences for captioning, limiting their practical application. This limitation typically arises due to two principal reasons: the simplicity and repetitiveness of the sentences in the datasets used for training models; and the relatively limited ability of these models to extract semantic features and generate complex descriptions.

The Large Language Models (LLMs) and Vision Language Models (VLMs) have recently achieved significant success across multiple fields, including computer vision [8], natural language processing [9], and robotics [10]. Particularly, VLMs [11], [12], [13] have effectively narrowed the gap between visual images and textual natural language by advancing the understanding of intermodal relationships, reaching a level of visual comprehension comparable to human capabilities. Therefore, some researchers [14], [15], [16], [17], [18], [19], [20] have recently shifted their focus to applying VLMs to remote sensing visual interpretation tasks. Specifically, for RSIC tasks, the RSGPT [15] introduced the human-annotated RSICap dataset, which provides high-quality and

detailed descriptions for remote sensing images. The remote sensing captions in this dataset include summarized scene descriptions, object information (color, shape, and count), and object relationships (relative position). However, RSGPT merely fine-tunes an existing VLM model on this dataset without proposing a novel model to explore and utilize the provided detailed descriptions deeply.

In this paper, we propose a novel Vision-Language Model (VLM) based on the Mixture of Experts (MoE) framework, named RS-MoE, specifically customized for the Remote Sensing Image Captioning (RSIC) task. To the best of our knowledge, this is the first work that applies the MoE framework to VLMs in the remote sensing domain. We extend the core principles of MoE to specifically address the unique challenges of remote sensing images. By decomposing the RSIC task into specialized subtasks, we leverage different expert models to facilitate more precise and contextually aware caption generation. Specifically, RS-MoE consists of three key components: the Image Encoder, the VLM Encoder, and the MoE Block. Unlike conventional MoE modules, our MoE Block consists of **a novel Instruction Router and multiple lightweight LLMs**. The Instruction Router is designed to generate tailored prompts for each LLM. In our experiments, these prompts focus on theme comprehension, object recognition, and relationship inference. The Instruction Router dynamically adjusts prompts based on visual features and task instructions, offering a more precise level of control and enabling the model to generate descriptions specifically tailored to each captioning objective. Furthermore, unlike traditional MoE models that typically use feed-forward networks (FFNs) as experts, we incorporate lightweight LLMs as expert models. This design allows each LLM to process complex, task-specific linguistic information efficiently and generate detailed, contextually aware descriptions while ensuring computational feasibility. In addition to the RS-MoE model, we propose a **two-stage training strategy** to fine-tune the MoE framework for the RSIC task, addressing potential model degradation caused by the sparsity that typically arises when applying MoE to remote sensing images. This sparsity arises from the lack of representation of remote sensing-specific features in models pretrained on natural images, leading to inefficiencies in capturing the complex characteristics of remote sensing imagery, which ultimately affects model performance. Moreover, to significantly reduce the number of trainable parameters, we incorporate the Low-Rank Adaptation (LoRA) training strategy into the RS-MoE tuning stages. After fine-tuning our model on the RSICap dataset using our proposed training strategy, we evaluated it on the RSICap dataset and directly tested it on traditional datasets, such as UCM-Captions, Sydney-Captions, and RSICD, without any additional fine-tuning on these datasets. Experimental results demonstrate that our RS-MoE-7B model achieves state-of-the-art performance, while the RS-MoE-1B variant achieves performance comparable to 13B VLMs in generating precise and contextually relevant captions. Furthermore, we extend our model to the Remote Sensing Visual Question Answering (RSVQA) task and demonstrate promising generalization capabilities by consistently achieving state-of-the-art performance on this task. Our contributions are

summarized as follows:

- We are the first to introduce the MoE framework within the domain of remote sensing. By drawing on the idea behind MoE for handling complex tasks through task decomposition, we break down the intricate challenges of remote sensing image captioning into distinct subtasks, enabling specialized expert models to more effectively address the diversity and complexity inherent in remote sensing data.
- We propose a novel Vision-Language Model, RS-MoE, specifically designed for remote sensing image captioning. Unlike traditional MoE models, our model introduces two key innovations: a novel Instruction Router module that dynamically generates task-specific prompts and lightweight LLMs as expert models. These innovations optimize the model's ability to handle the complexity and diversity of remote sensing images while maintaining computational efficiency.
- We present a two-stage training strategy for the RS-MoE model tailored to the RSIC task, which incorporates a proper initialization process to prevent model degradation due to the sparsity that typically results from directly applying MoE. Additionally, we employ the LoRA technique to significantly reduce the number of trainable parameters, thereby enhancing the efficiency and manageability of the model during the training process.
- Extensive experiments demonstrate that, even with fine-tuning on only one dataset containing around 3,000 images, our model achieves state-of-the-art performance across four RSIC datasets and exhibits strong generalization capabilities on an RSVQA dataset. Notably, our lightweight RS-MoE-1B model achieves comparable performance to larger 13B VLM methods for remote sensing image captioning, while offering significantly greater efficiency.

II. RELATED WORK

A. Remote Sensing Image Captioning

Remote Sensing Image Captioning (RSIC) poses a challenging task within the fields of computer vision and specialized linguistic modeling, aiming to generate descriptive narratives for remote sensing images by focusing on their visual attributes. Early methodologies predominantly employed template-based [1] and retrieval-based techniques [2], [3]. Template-based strategies involve creating fixed sentence structures and populating them with relevant information, such as attributes and categories displayed within the image. Conversely, retrieval-based strategies develop large-scale databases containing images and their corresponding textual descriptions. These strategies retrieve the most similar image from the database and provide the corresponding description.

Recent studies [4], [5], [6], [7] have proposed methods based on the Encoder-Decoder framework for achieving RSIC tasks. This architecture typically incorporates an image encoder to extract semantic features from images, which are then interpreted by a sequential model to produce textual annotations. Depending on the model used for the encoder,

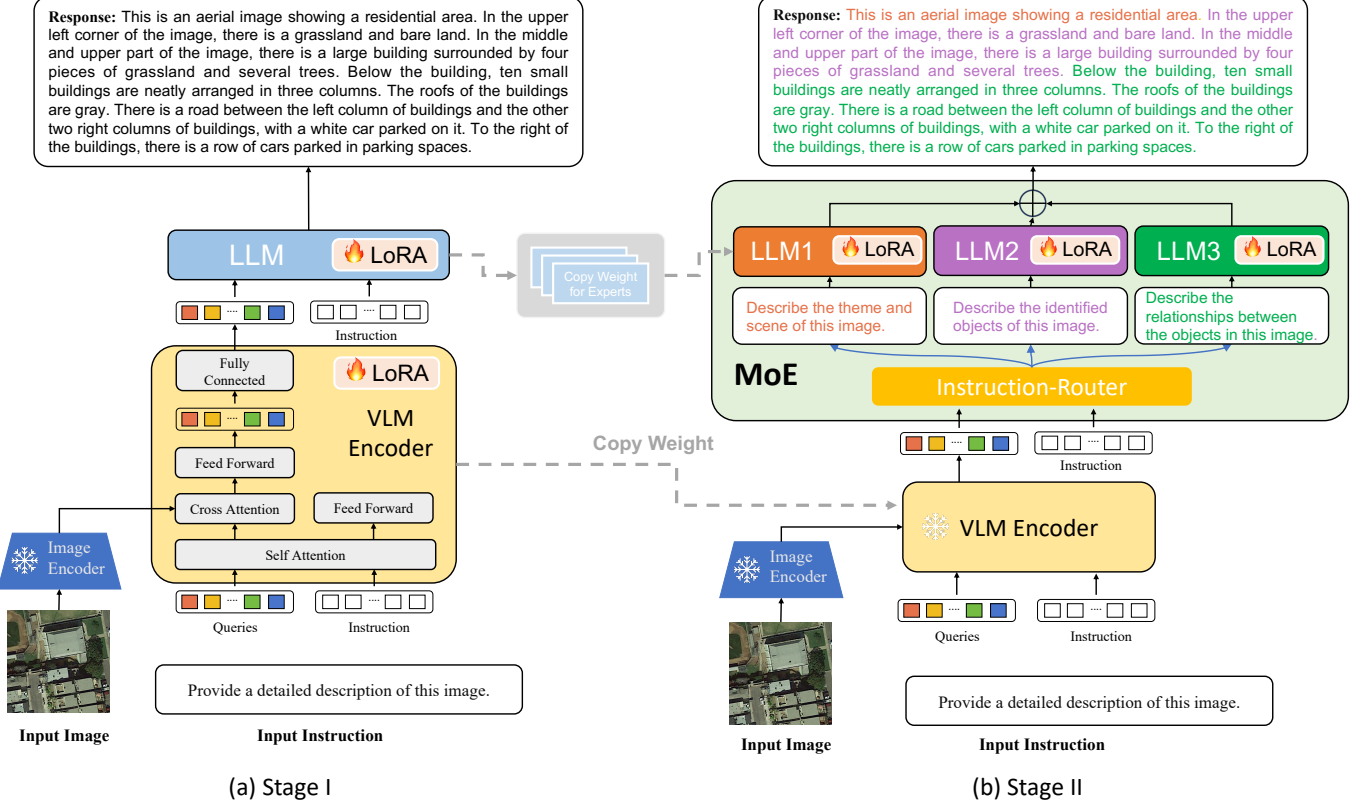


Fig. 1. Overview of the proposed RS-MoE model, which consists of three key components: the Image Encoder, the VLM Encoder, and the MoE Block. The MoE Block comprises an Instruction Router that dynamically generates task-specific prompts and three lightweight LLMs, which focus on different aspects of the captioning task. In the generated captions, shown in the top right corner of the figure, distinct colors represent each aspect: orange for the overall theme, purple for specific objects, and green for relationships between objects. RS-MoE is trained using a novel two-stage training strategy specifically designed for remote sensing image captioning. In Stage I (a), the VLM Encoder and the LLM Block are fine-tuned to initialize model weights specifically designed for the RSIC task. In Stage II (b), the MoE Block is fine-tuned to produce more detailed captions for RSIC tasks.

existing Encoder-Decoder methodologies for RSIC can be categorized into two types: CNN-based image encoders with RNN-based text decoders, and CNN-based image encoders with Transformer-based text decoders. For instance, [4] first fine-tuned the CNN alongside the VAE in the first phase, followed by employing both Transformer and Reinforcement Learning to process spatial and semantic features for text generation. To incorporate the domain-specific knowledge of remote sensing, [5] introduced a fine-grained and structured attention-based model that capitalizes on the structural attributes of semantic content in high-resolution RS images. Besides, [6] first implemented a multi-scale visual feature encoder to extract detailed information from RS images and then engaged an adaptive multi-head attention decoder to refine the text generation process based on the extracted multi-scale features.

More recently, some researchers have begun to explore the use of VLM for the RSIC task. [7] introduced a vision-language aligning network that utilizes CLIP for visual feature extraction and a pretrained generative language model, GPT-2, to generate relevant descriptions for given remote sensing images. Additionally, [15] have developed a high-quality, human-annotated remote sensing image captioning dataset with detailed and rich descriptions specifically for the RSIC

task, as well as an evaluation dataset for assessing general VLMs. They further fine-tuned the Instruct-BLIP model on this dataset, establishing a benchmark for both RSIC and RSVQA tasks.

B. VLM in Remote Sensing

Vision-Language Models (VLMs) [11], [12], [13] are cutting-edge frameworks designed to integrate visual and textual modalities, enabling models to effectively interpret and generate both visual content and corresponding linguistic descriptions. These models have demonstrated significant advancements in tasks involving natural images, especially in generating dialogues and interpreting visual data. By combining visual features with contextual cues, VLMs provide a more interactive and coherent understanding of visual inputs. For instance, the LLaVA model [21] exemplified both data efficiency and architectural simplicity by employing a fully connected vision-language projection layer, enabling multimodal understanding using only 600K image-text pairs. More recently, Qwen2-VL [22] introduced a dynamic resolution mechanism alongside Multimodal Rotary Position Embedding M-RoPE, which allows the model to process images of varying resolutions, substantially improving accuracy and flexibility in multimodal tasks.

Inspired by the rapid advancements in computer vision, researchers have increasingly focused on integrating Vision-Language Models (VLMs) into remote sensing tasks. One of the early comprehensive reviews, [23], highlighted key VLM applications within the remote sensing domain, identifying both the current challenges and future directions for research. Since then, several VLM-based models have emerged to address these challenges. For example, [18] introduced Earth-GPT, a model specifically designed for multi-sensor remote sensing image interpretation. This model integrates three core innovations: vision-enhanced perception, cross-modal understanding, and a unified instruction tuning mechanism, making it particularly effective for handling complex remote sensing data. In addition to these novel approaches, many remote sensing VLMs build upon the foundational architecture of LLaVA, adapting it to better address the specific challenges of remote sensing. RS-LLaVA enhances the standard LLaVA framework by incorporating a low-rank adaptation (LoRA) mechanism, optimizing the model's ability to process the multi-scale and high-resolution nature of remote sensing images while maintaining computational efficiency. Similarly, H2RSVLM extends LLaVA by integrating a pretrained vision encoder and LLM, connected through a multilayer perceptron (MLP) projector. This model is particularly designed to improve its handling of complex queries and mitigate incorrect generations, especially in remote sensing contexts where "hallucinations" are a common issue. GeoChat, also based on LLaVA, incorporates task-specific prompts and spatial capabilities, enabling it to handle multiple remote sensing tasks more effectively. These enhancements allow the model to better understand visual prompts and generate grounded object descriptions, providing more detailed and context-specific interactions in response to image and region-level queries.

III. METHODS

A. Problem Statement

Let $I \in \mathbb{R}^{W \times H \times 3}$ be a remote sensing image, where W and H denote the width and height of the image, respectively, and the 3 represents the RGB color channels. The objective of RSIC is to generate a descriptive caption $S = \{s_1, \dots, s_n\}$, where each s_i is a sentence that effectively summarizes the content of the image. Consider $\mathcal{O} = \{o_1, o_2, \dots, o_m\}$ as the set of visible geographic objects within I , where each o_j represents an object identified in the remote sensing image. The relationships among these objects can be denoted as \mathcal{R} , where $\mathcal{R} \subseteq \mathcal{O} \times \mathcal{O}$ represents a set of tuples (o_i, o_k) , indicating a significant interaction or spatial relationship between object o_i and object o_k . An effective captioning model for RSIC should not only **identify the objects** in \mathcal{O} but also **interpret the relationships** in \mathcal{R} .

B. Model Architecture

As shown in Figure 1, the proposed RS-MoE model consists of four modules, including an Image Encoder, a Vision Language Model (VLM) Encoder, a Large Language Model (LLM) Block, and a Mixture of Experts (MoE) Block.

1) *Image Encoder*: Given a remote sensing image I , we first employ an Image Encoder f_I to extract the visual feature F_I . We adopt the ViT-G/14 [24], a large Vision Transformer that contains nearly two billion parameters, as our image encoder. We freeze this visual backbone during the entire model training process.

2) *VLM Encoder*: Inspired by the InstructBLIP [13], our VLM Encoder, denoted as f_{VLM} , is specifically designed to extract visual features that are attuned to the given instructions T . Firstly, a series of learnable query embeddings, along with corresponding instructions, are fed into the self-attention layers of the VLM Encoder, yielding an intermediate feature set F_{SA} . Subsequently, these features, together with the visual features F_I derived from the Image Encoder, are processed through cross-attention layers. This step is pivotal for synthesizing the instruction-aware visual features F_{CA} , which are tailored to be both adaptable and insightful based on the input instructions. Finally, the feature set F_{CA} progresses through a feed-forward network, culminating in a fully connected layer that outputs the refined feature representation F_{VLM} .

3) *LLM Block*: The learned instruction-aware features F_{VLM} and the corresponding instructions T serve as input prompts to the LLM Block f_l , facilitating the generation of detailed and coherent natural language captions S . This LLM Block is used during the first training stage of our model to set up and initialize the weights of the LLM models within the MoE Block for next training stage.

4) *MoE Block*: Unlike traditional MoE modules, the MoE Block comprises a novel instruction-router, the MoE Block comprises an Instruction-router R and N distinct Large Language Models (LLMs), denoted as $\{f_{l1}, f_{l2}, \dots, f_{lN}\}$. The instruction-router R is designed to generate N detailed prompts based on the input instruction T , represented as $\{P_1, P_2, \dots, P_N\}$. Its design is grounded in the principles of Prompt Learning, adapting to various characteristics of the input image and dynamically generating prompts related to visual features to guide the expert models in producing targeted descriptions. During training, it learns how to dynamically adjust prompts based on visual features and task instructions, thereby more effectively guiding each expert model's generation process. This enables the model to adapt to different image features and generate more precise and detailed descriptions.

The prompts generated by the instruction-router are then directed to their respective LLMs, each with the precise objective of focusing the LLM on a specialized sub-task. This targeted approach enables each LLM to concentrate on a specific aspect of the input data, allowing the model to develop a deep, focused expertise within a defined domain. Specifically, we break down the caption generation task into three specialized subtasks, assigning each LLM to one of the following areas: thematic interpretation, object identification, and the analysis of object relationships. By distributing these distinct sub-tasks to separate LLMs, the model effectively reduces the complexity of the captioning task into more manageable components, allowing each LLM to excel in solving its designated aspect of the task. This modular design enhances precision, as each LLM specializes in a narrower

scope, reducing the risk of generalization errors. Additionally, this specialization allows for more nuanced control over the model’s outputs. The instruction-router dynamically adjusts prompts based on the context, ensuring that each LLM is aligned with the most relevant and accurate information for its sub-task. Ultimately, this framework enhances the model’s overall performance by leveraging the collective expertise of multiple LLMs, each optimized for a particular sub-task in the caption generation process.

C. Model Tuning

As illustrated in Figure 1, the tuning process of the proposed RS-MoE model is divided into two stages. Considering the complexity and diversity of information within remote sensing images, directly training our model can lead to performance degradation due to sparsity. This sparsity stems from the inadequate representation of remote sensing-specific features in models pre-trained on natural images, creating inefficiencies in capturing the intricate characteristics of remote sensing imagery, ultimately impacting model performance. To address this, we propose a two-stage training strategy. The first stage begins by independently training the VLM Encoder and LLM, ensuring that the encoder can extract rich and detailed visual features specific to remote sensing imagery while enhancing its capability to generate meaningful, context-aware feature representations. Once the VLM Encoder generates stable visual features, the second stage involves fine-tuning the language models in the MoE. In this stage, focus shifts to adjusting the MoE Block’s weights to produce more detailed captions tailored specifically for RSIC tasks, with each language model concentrating on its designated task.

1) *Stage I*: In this stage, our primary focus is on tuning the weights of the VLM Encoder and the LLM Block to initialize model weights specifically designed for the RSIC task. Specifically, we freeze the Image Encoder and then train the VLM Encoder based on the extracted visual features and input instructions. This tuning enhances the encoder’s ability to associate specific visual features with relevant instructional information, thereby improving its capability to generate meaningful and context-aware feature representations from remote sensing images. To significantly reduce the number of trainable parameters, we incorporate the LoRA training strategy during the VLM Encoder training stage. Firstly, within the self-attention layers, LoRA is specifically applied to the query and value projection layers. Secondly, LoRA is also implemented across all projection layers within the cross-attention layers, including those for the query, key, value, and output. Thirdly, LoRA is integrated into the feed-forward network components, ensuring a comprehensive application of this strategy throughout the model.

The LLM block receives output features and instructions from the instruction-aware VLM Encoder to generate the final captions for remote sensing images, which plays a crucial role in synthesizing the contextual data provided by the VLM Encoder into coherent and detailed textual descriptions. The fine-tuning process is focused on enhancing the model’s ability to understand the complex visual patterns typical of remote

sensing images and to translate them into accurate linguistic representations. By tuning the LLM Block, the model becomes more efficient at generating captions that are deeply aligned with the specific requirements of remote sensing tasks, including adapting to various landscapes, recognizing subtle environmental changes, and describing intricate relationships between different geographical features in the images. Similarly, we employ the LoRA technique to reduce the number of trainable parameters, thereby enhancing the model’s efficiency and manageability during the training process. LoRA is specifically applied to the query and value layers within the attention module, as well as to the feed-forward networks. This optimization not only streamlines the training process but also sharpens the focus of the attention mechanisms, improving the overall processing and responsiveness of the model.

2) *Stage II*: In this stage, our focus shifts to fine-tuning the MoE Block’s weights to produce more detailed captions specifically for remote sensing image captioning tasks. Tuning the MoE Block involves detailed adjustments to the interaction mechanisms between the distinct LLMs to ensure that each LLM can effectively respond to its specific prompt by extracting and interpreting nuanced visual cues. This fine-tuning facilitates the development of a deep, segmented understanding of the image, allowing each expert within the MoE to generate a part of the caption that reflects its specialized knowledge of the image’s theme, objects, or relationships. As these parts come together, they form a comprehensive and detailed caption that captures both the breadth and depth of the remote sensing imagery.

Specifically, we freeze the Image Encoder and the VLM Encoder, where the weights of the VLM Encoder are copied from those trained in Stage I. The MoE Block uses the Instruction Router to convert the instruction into specific prompts, which are then combined with the features extracted by the VLM Encoder related to the remote sensing images and input into different LLMs. By tuning the MoE, which principally involves tuning each of the sub-LLM Blocks within it, we initialize the weights of each LLM Block using the weights from the LLM Blocks that were trained in Stage I. During the tuning process, we continue to employ the LoRA training strategy to further enhance the models’ efficiency and effectiveness. This approach not only streamlines the training by reducing the number of parameters that need to be tuned but also assists in fine-tuning the model’s ability to concentrate on specific features of the input data, thereby enhancing the overall accuracy and responsiveness of our system.

IV. EXPERIMENTS

A. Datasets

1) *RSICap*: This dataset is built on the DOTA object detection dataset, which contains 2,585 high-quality remote sensing image-text pairs for training vision-language models on remote sensing images. The images are randomly chosen from the DOTA dataset and resized to 512×512 pixels. The text annotations are manually labeled by five experts in the remote sensing field. To evaluate the VLM model on this dataset, the authors further constructed an evaluation

set, RSIEval, that consists of 1,000 512x512 remote sensing images with manual annotations.

a) UCM-Captions: This dataset is derived from the UC Merced Land Use Dataset. It consists of 2,100 remote sensing images, categorized into 21 land use classes, each containing 100 images. Each image measures 256×256 pixels, with a pixel resolution of 0.3048 meters. The image captions were manually extracted from large-scale images provided by the United States Geological Survey's National Map Urban Area Imagery. Each image is described by five sentences, which are relatively fixed in structure and simple in their descriptions

b) Sydney-Captions: This dataset is constructed from the Sydney Data Set. It comprises 613 remote sensing images divided into 7 land use categories. Each image measures 500×500 pixels, with a pixel resolution of 0.5 meters. Each image is described in five sentences.

c) RSICD: This dataset contains 10,921 remote sensing images collected from four platforms: Google Earth, Baidu Maps, MapABC, and Tianditu. The images are uniformly resized to 224×224 pixels, although they come in various resolutions. The captions for these images were created by volunteers who possess experience in annotation and knowledge of remote sensing. For each image, the original caption varies from one to five sentences. To enrich the descriptions, the authors duplicated the captions that contained fewer than five sentences to ensure that each image had five distinct sentences in its caption.

B. Evaluation Metrics

BiLingual Evaluation Understudy (BLEU) operates by comparing the text generated by the model to reference texts that are considered correct. BLEU examines the presence and frequency of n-grams in the generated text that appears in the reference text and calculates a score based on the precision of these n-grams. We tested BLEU scores for n-grams of sizes 1, 2, 3, and 4.

Recall-Oriented Understudy for Gisting Evaluation (ROUGE-L) is a metric designed to evaluate the quality of summaries by measuring the longest common subsequence (LCS) between the generated text and the reference text. In the context of image captioning, ROUGE-L assesses the extent to which the content of a generated caption overlaps with that of a set of reference captions. This metric is recall-oriented, focusing on the coverage provided by the generated caption of the reference captions.

Metric for Evaluation of Translation with Explicit Ordering (METEOR) is an evaluation metric that considers not only the precision but also the recall of matched words between the generated text and reference texts, thus balancing accuracy and coverage. It also accounts for synonymy and stemming, allowing for a more nuanced comparison of content.

Consensus-based Image Description Evaluation (CIDEr) is specifically developed for scoring image captions by comparing them to reference captions written by humans. It measures the consensus between a candidate caption and the set of reference captions. This metric evaluates the similarity of n-grams between the generated and reference captions,

weighting more frequent n-grams higher to reflect their importance in the descriptions.

C. Experimental Details

We trained our model on 3 NVIDIA A100 GPUs, each with 80GB of memory. We selected three distinct versions of LLMs for use in our MoE model: Llama-3.2-1B [27], Llama-3.2-3B [27], and Vicuna-7B [28]. Each LLM within the MoE Block was individually fine-tuned for only 5 epochs. During the training process, the learning rate was initially set to $1e-4$, and a warm-up phase for the learning rate was applied for one epoch. We used the AdamW optimizer with parameters set to $\beta_1 = 0.9$, $\beta_2 = 0.999$, and a weight decay of 0.05, alongside adopting a cosine decay schedule for the reduction of the learning rate.

D. Results

1) Results on RSICap: We first evaluated the proposed RS-MoE model against state-of-the-art VLMs on the RSICap dataset for the Remote Sensing Image Captioning task. Since these VLMs were initially designed for natural images, we fine-tuned each model according to the training strategies specified in their respective papers to ensure optimal adaptation for remote sensing tasks. To ensure a fair comparison, all models were fine-tuned for 5 epochs, aligning with the training regime of our RS-MoE. Subsequently, we tested all models, including three versions of RS-MoE, on the RSIEval dataset to assess their captioning accuracy. The results, displayed in Table I, demonstrate that our RS-MoE-7B model outperformed other models across all seven evaluation metrics, including four BLEU score variants, as well as METEOR, ROUGE-L, and CIDEr scores.

Notably, our two lightweight variants, RS-MoE-1B and RS-MoE-3B, achieved performance comparable to the larger 7B and 13B state-of-the-art models and even outperformed them on certain metrics. For instance, RS-MoE-1B exceeded BLIP2-13B in BLEU-1, METEOR, ROUGE-L, and CIDEr scores. Additionally, RS-MoE-1B not only surpassed BLIP2-13B but also outperformed MiniGPT4-13B and InstructBLIP-13B on the METEOR metric. These findings highlight the remarkable efficiency of our smaller models, as RS-MoE-1B and RS-MoE-3B deliver competitive performance while requiring significantly fewer parameters than their larger counterparts. Such compact architectures are particularly advantageous for resource-constrained environments, as they offer reduced computational overhead and are ideal for deployment in practical settings with limited memory and processing power.

Overall, the RS-MoE model demonstrates exceptional efficiency and accuracy in addressing the RSIC task. By leveraging its innovative architecture, including the MoE framework and specialized training strategy, the model effectively captures and interprets the complex visual information inherent in remote sensing images. This allows for the generation of precise, contextually relevant captions. Thus, our model not only excels in terms of performance but also proves highly practical for real-world applications, especially in environments where computational resources are limited.

BLIP2: A satellite image of a city street with cars and buildings.



MiniGPT4: This is a satellite image of a neighborhood in the city of San Diego, California. The neighborhood is made up of single-family homes with pools in the front yard. The houses are surrounded by trees and greenery. The streets are lined with palm trees and there

InstructBLIP: An image of a residential neighborhood with many houses lined up in a grid-like pattern. There are several swimming pools visible in the yards of the houses, as well as several cars parked on the streets. There is a road running through the middle of the neighborhood. The houses are surrounded by trees and shrubs, and there are some palm trees visible in the background.

RSGPT: This is an image of a residential neighborhood with many houses and swimming pools. There are a total of nine swimming pools visible in the image. The houses are well-maintained, and the swimming pools are clean and clearly visible. There are also several trees scattered throughout the neighborhood, and some of them are located near the swimming pools. A road runs through the center of the

RS-MoE: This is an image of a well-maintained residential neighborhood with many houses and swimming pools. There are many houses in the neighborhood, almost all of them have swimming pools. There are a total of twelve swimming pools visible in the image. In addition to the swimming pools, there are also several cars parked in the driveways of the houses. There is a road running through the middle of the neighborhood, and a power line runs around it. There are also several trees scattered throughout the neighborhood.

BLIP2: A satellite image of an industrial area with many trees.



MiniGPT4: The image shows a satellite view of a large industrial complex with several large tanks and other buildings. The tanks appear to be white and cylindrical in shape, with some smaller tanks.

InstructBLIP: This is a satellite image of an industrial area. There are several large white storage tanks in the center of the image, surrounded by trees and other buildings. There is a road running along the left side of the image, and a smaller road running along the right side. In the foreground, there is a wooded area.

RSGPT: This is a satellite image of an industrial area. There are some large white buildings. There is a road running along the bottom of the image, and a smaller road branching off to the left. There is also a small body of water visible in the top right corner of the image. Overall, the image depicts an industrial area with several large storage tanks and various other buildings.

RS-MoE: This is a satellite image of an industrial area. There are several large white storage tanks in the left corner of the image, surrounded by trees and other buildings. There is a road running along the left side of the image, and a smaller road running along the right side. There is a forest in the right side of the image. There are some storage tanks to the left of the forest. A road runs through the middle of the industrial area, above the road there are many small storage tanks, below the road is a large storage tank.

BLIP2: An aerial image shows an rural area.



MiniGPT4: The image shows a satellite view of farmland. There is farmland surrounded by many trees, and there are some houses next to the farm. There is a parking lot with some cars in it.

InstructBLIP: This image is an aerial view of a rural area with a river running through it. There are trees on either side of the river, and there are some buildings visible in the distance. In the foreground, there is a field with crops growing in it. There is a road running along the edge of the field, and there are some vehicles on the road. In the lower left corner of the image, there is a small parking lot with several cars parked in it. There is also a building visible in the lower left corner. Overall, the image shows a peaceful, rural landscape with a mix of natural and man-made features.

RSGPT: This is an aerial image of a rural area. There is a river running through the center of the image, with trees and shrubs growing along its banks. On the left side of the image, there is a road running parallel to the river. There are some buildings visible in the distance. In the foreground, there is a small parking lot with several cars parked in it. There are also some utility poles and power lines running along the road. Overall, the image shows a peaceful, rural landscape with a mix of natural and man-made features.

RS-MoE: This is an aerial image of a rural area with a river running through it. There is a lot of green vegetation in the area, including trees and grass. There is also a parking lot with several cars parked in it. In the upper right of the image, there is a field with some kind of crop growing in it. There is a road next to the river. There are several buildings on the left side of the road and there is a farm on the right side of the road. There is a farm surrounding by trees, and there is some crops in the farm.

Fig. 2. Qualitative results of image captions generated by our RS-MoE model and the SOTA model for three randomly selected remote sensing images from the RSEval dataset. In captions generated by our model, different colors indicate distinct aspects of the image: orange for the overall theme, purple for objects within the scene, and green for spatial relationships between objects.

TABLE I
RESULTS OF OUR MODEL AND STATE-OF-THE-ART MODELS ON THE RSIEVAL DATASET FOR RSIC TASK.

Method	BLEU-1	BLEU-2	BLEU-3	BLEU-4	METEOR	ROUGE_L	CIDEr
BLIP2-13B [11]	54.51	42.42	34.64	28.17	27.54	24.38	105.51
MiniGPT4-13B [12]	68.49	59.31	43.22	39.78	31.70	30.95	120.33
InstructBLIP-13B [13]	63.71	50.76	49.35	40.50	30.58	27.15	121.91
RSGPT-13B [15]	77.05	62.18	48.25	40.34	37.41	33.26	149.32
Qwen2-VL-7B [25]	78.66	60.98	47.07	39.24	40.05	32.63	124.36
LLaVA-NeXT-7B [26]	81.72	63.99	49.31	40.38	39.59	34.62	128.27
RS-MoE-1B	57.36	42.25	22.14	20.54	32.36	25.98	109.37
RS-MoE-3B	65.11	52.44	28.78	26.86	40.04	27.62	120.20
RS-MoE-7B	82.13	65.44	51.93	42.55	40.28	35.72	158.36

TABLE II
RESULTS OF OUR MODEL AND STATE-OF-THE-ART MODELS ON THE UCM-CAPTIONS DATASET FOR RSIC TASK.

Method	BLEU-1	BLEU-2	BLEU-3	BLEU-4	METEOR	ROUGE_L	CIDEr
VLAD + RNN [29]	63.11	51.93	46.06	42.09	29.71	58.78	200.66
VLAD + LSTM [29]	70.16	60.85	54.96	50.30	34.64	65.20	231.31
mRNN [30]	60.10	50.70	32.80	20.80	19.30	-	214.00
mLSTM [30]	63.50	53.20	37.50	21.30	20.30	-	222.50
mGRU [31]	42.56	29.99	22.91	17.98	19.41	37.97	124.82
mGRU embedword [31]	75.74	69.83	64.51	59.98	36.85	66.74	279.24
CSMLF [32]	37.71	14.85	7.63	5.05	9.44	29.86	13.51
SAA [33]	79.62	74.01	69.09	64.77	38.59	69.42	294.51
Soft-attention [34]	74.54	65.45	58.55	52.50	38.86	72.37	261.24
Hard-attention [34]	81.57	73.12	67.02	61.82	42.63	76.98	299.47
SD-RSIC [35]	74.80	66.40	59.80	53.80	39.00	69.50	213.20
RTRMN (semantic) [36]	55.26	45.15	39.62	35.87	25.98	55.38	180.25
RTRMN (statistical) [36]	80.28	73.22	68.21	63.93	42.58	77.26	312.70
SVM-D BOW [37]	76.35	66.64	58.69	51.95	36.54	68.01	271.42
SVM-D CONC [37]	76.53	69.47	64.17	59.42	37.02	68.77	292.28
Post-processing [38]	79.73	72.98	67.44	62.62	40.80	74.06	309.64
RSGPT-13B [15]	86.12	79.14	72.31	65.74	42.21	78.34	333.23
SkyEyeGPT-7B [39]	90.71	85.69	81.56	78.41	46.24	79.49	236.75
RS-LLaVA-13B [40]	90.00	84.88	80.30	76.03	49.21	85.78	355.61
RS-CapRet-7B [41]	84.30	77.90	72.20	67.00	47.20	81.70	354.80
RS-MoE-7B w/o finetuning	94.81	87.09	79.57	72.34	66.97	62.74	396.46

To more intuitively compare the captioning performance of our model with other models for given remote sensing images, we randomly selected three images from the RSIEval dataset and listed the captions generated by each model in Figure 2. These three images represent three distinct scenes: urban streets, industrial areas, and rural regions. By comparing the results of the generated captions from different models, several key findings can be made. The BLIP2 model provides relatively simple image captions, focusing mainly on the primary objects in the remote sensing images. The MiniGPT4 and InstructBLIP models incorporate more details and contextual

information in their descriptions, such as trees around houses, swimming pools, and roads. These details enrich the descriptions but can sometimes result in information redundancy. The RSGPT model describes the images in a more structured manner. However, some of its generated descriptions may lack accuracy, such as the number of swimming pools, and may include some subjective and hallucinatory sentences. Conversely, our RS-MoE model describes the images with clear logic from three perspectives: themes, objects present, and the relationships between objects. The RS-MoE model provides more accurate descriptions of the types, quantities,



RSGPT: An image of a densely populated residential area with many trees and parking lots. The area is surrounded by a road, and there is a traffic light at one of the intersections. Some of the buildings have solar panels on their roofs. There are several cars parked in the parking lots, and a few people can be seen walking around the area. The image is in color and has a high level of detail. It is a clear day, and the sun is shining brightly. The image is captured from an oblique angle, looking down onto the area. The terrain is relatively flat, and there are no notable landmarks or bodies of water in the vicinity. The image can be used to showcase the features and characteristics of the residential area, such as its density, greenery, and modern amenities. It can'

RS-MoE: This image is an aerial view of a residential neighborhood. There are many residential buildings. There is a swimming pool in the right upper corner of the image. In the lower right of the image, there is a parking lot and there are many cars in it. There is a road to the upper left of the residential area. These houses are surrounded by many trees. There is a swimming pool surrounding by buildings. All the houses have grey roofs and it is a very tightly arranged residential area.



RSGPT: This is a image of an airport. There are many planes in the image and there is a terminal in the image. The plane is surrounding by many cars. There is an airstrip on the right side of the image. The overall scene appears to be a busy airport with multiple planes and vehicles present. The image is clear and detailed, allowing for easy identification of the various objects present.

RS-MoE: This is a thermal satellite image of an airport. There's a white plane in the middle of the image. There is a terminal in the upper of the image. There are also some smaller buildings and other structures visible in the image. There is a plane parked at the terminal, and a few cars and trucks are visible near the planes. There is a large white building next to the planes, which appears to be a terminal or hangar.

Fig. 3. Qualitative results of image captions generated by RSGPT and our RS-MoE model for two randomly selected remote sensing images from the UCM-Captions dataset. In captions generated by our model, different colors indicate distinct aspects of the image: orange for the overall theme, purple for objects within the scene, and green for spatial relationships between objects.

and spatial relationships of the objects present in images.

2) *Results on UCM-Captions:* We further validated the performance of our model on the classic UCM-Captions dataset. To establish a comprehensive comparison, we selected sixteen deep learning models specifically designed for the RSIC task, representing state-of-the-art approaches in remote sensing image captioning prior to the advent of VLM models. Additionally, we evaluated recent state-of-the-art VLM models in the remote sensing domain, including RSGPT [15], SkyEyeGPT [39], RS-LLaVA [40], and RS-CapRet [41]. Notably, we evaluated the performance of the 7B version of RS-MoE, which was trained on the RSICap dataset **without any additional fine-tuning** on the UCM-Captions dataset. The comparative results of these baseline models and our model are presented in Table II. Remarkably, even without fine-tuning on the UCM-Captions dataset, our model achieved the highest performance across several metrics, including BLEU-1, BLEU-2, METEOR, and CIDEr. Specifically, our model achieved a METEOR score of 66.97, significantly surpassing the second-highest score of 49.21 obtained by the RS-LLaVA-13B model, further demonstrating the robustness and generalizability of RS-MoE across different datasets.

To further illustrate the effectiveness of our model in generating accurate and contextually aware captions, we selected two remote sensing images with distinct scenes from the test set of the UCM-Captions dataset. The captions generated by RSGPT and our model for these images are shown in Figure 3. As observed, both models successfully capture the overall themes of the images. However, for detailed descriptions, particularly in the first remote sensing image, the captions generated by RSGPT exhibit discrepancies with the actual scene. In contrast, the captions produced by the proposed

RS-MoE model provide precise and detailed representations of both the objects and their spatial relationships within the remote sensing images, underscoring our model's advantage in understanding complex spatial arrangements in diverse remote sensing imagery.

3) *Results on Sydney-Captions:* To further assess our model's efficacy for the RSIC task, we extended the evaluation to the traditional Sydney-Captions dataset. In this experiment, sixteen deep learning models specifically designed for remote sensing image captioning, along with two recent VLM models, RSGPT [15] and RS-CapRet [41], were selected as comparative benchmarks. Noted that we still employed the 7B variant of RS-MoE **without any additional fine-tuning** on the Sydney-Captions dataset. The comparative performance of these baseline models and our model is detailed in Table III. Analysis of the results demonstrates that, even without fine-tuning, our model consistently outperformed all competing models across all seven evaluation metrics. A particularly notable achievement is its performance on the METEOR metric, where it achieved a score of 56.23, surpassing the next best model, which scored 41.37, by a substantial margin of 15%.

To further illustrate the captioning capabilities of our model in comparison to RSGPT, we randomly selected two remote sensing images from the test set of the Sydney-Captions dataset, as shown in Figure 4. These images depict scenes of a residential area and an airport. Figure 4 shows that while both RSGPT and RS-MoE provide generally accurate descriptions of the overall themes and specific details, the RSGPT-generated captions lack the depth observed in our model's outputs. Additionally, the last sentence generated by RSGPT for the first image remains incomplete, underscoring

TABLE III
RESULTS OF OUR MODEL AND STATE-OF-THE-ART MODELS ON THE SYDNEY-CAPTIONS DATASET FOR RSIC TASK.

Method	BLEU-1	BLEU-2	BLEU-3	BLEU-4	METEOR	ROUGE_L	CIDEr
VLAD + RNN [29]	56.58	45.14	38.07	32.79	26.72	52.71	93.72
VLAD + LSTM [29]	49.13	34.12	27.60	23.14	19.30	42.01	91.64
mRNN [30]	51.30	37.50	20.40	19.30	18.50	-	161.00
mLSTM [30]	54.60	39.50	22.30	21.20	20.50	-	186.00
mGRU [31]	69.64	60.92	52.39	44.21	31.12	59.17	171.55
mGRU embedword [31]	68.85	60.03	51.81	44.29	30.36	57.47	168.94
CSMLF [32]	59.98	45.83	38.69	34.33	24.75	50.18	75.55
SAA [33]	68.82	60.73	52.94	45.39	30.49	58.20	170.52
Soft-attention [34]	73.22	66.74	62.23	58.20	39.42	71.27	249.93
Hard-attention [34]	75.91	66.10	58.89	52.58	38.98	71.89	218.19
SD-RSIC [35]	72.40	62.10	53.20	45.10	34.20	63.60	139.50
SVM-D BOW [37]	77.87	68.35	60.23	53.05	37.97	69.92	227.22
SVM-D CONC [37]	75.47	67.11	59.70	53.08	36.43	67.46	222.22
Post-processing [38]	78.37	69.85	63.22	57.17	39.49	71.06	255.53
RSGPT-13B [15]	82.26	75.28	68.57	62.23	41.37	74.77	273.08
RS-CapRet-7B [41]	78.70	70.00	62.80	56.40	38.80	70.70	239.20
RS-MoE-7B w/o finetuning	84.56	76.10	69.25	63.02	56.23	76.62	279.76



RSGPT: This is a satellite image of a densely populated urban area. There are many high-rise residential buildings, roads, and trees visible in the image. The area appears to be an inner-city suburb with a mix of houses and apartments. There are also several parks and green spaces visible in the image. The image also shows the mix of old and new buildings in the area, with some buildings appearing to be quite old while others are more modern. There are also several businesses and shops visible in the

RS-MoE: This is a satellite image of a residential area of the city. There are three large residential areas in the image. There are many buildings in the image. There are also several trees scattered throughout the neighborhood. In the middle of the image there is a car park with many cars parked in it. There are two roads on either side of the image that run through the entire residential area. There is a lot of cars are traveling. In the bottom left corner of the image residential are some white flats and at the bottom of the image there is a small park. This is a very busy residential area.



RSGPT: The image is an aerial view of an airport, showing several airplanes parked on the tarmac. There is a large white building in the center of the airport with several smaller planes parked around it. There is also a taxiway and a runway visible in the image. The image has a high level of detail and is labeled with the names of the different features visible in the scene.

RS-MoE: This image is an aerial view of an airport. There is a large building in the lower right corner of the image. To the left of the image is an airstrip and a grassy area. There is a lawn in the left side of the image. There are many planes surrounding the building. There is an airstrip in the upper right corner of the airport. There are also some vehicles parked inside the airport. All airplane and vehicles are surrounding the airport.

Fig. 4. Qualitative results of image captions generated by RSGPT and our RS-MoE model for two randomly selected remote sensing images from the Sydney-Captions dataset. In captions generated by our model, different colors indicate distinct aspects of the image: orange for the overall theme, purple for objects within the scene, and green for spatial relationships between objects.

our model’s advantage in generating coherent and contextually rich descriptions.

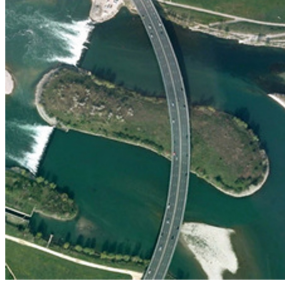
4) *Results on RSICD*: Finally, we validated the performance of our model on the widely used RSICD dataset for the RSIC task. Consistent with previous evaluations, we compared our model against sixteen deep learning models and two recent VLM models, RSGPT [15] and RS-CapRet [41], with our RS-

MoE-7B model evaluated **without additional fine-tuning** on the RSICD dataset. The comparative results for these baseline models and our model are presented in Table IV. As observed in Table IV, even without fine-tuning, our model achieved the highest scores on five out of seven metrics, including BLEU-1, BLEU-2, BLEU-3, BLEU-4, and METEOR. This highlights the robustness and adaptability of our approach, underscoring



RSGPT: This is a satellite image of an airport. There are several buildings and parking lots visible, as well as a runway and taxiways. There are also some trees and a body of water near the airport. The surrounding area appears to be mostly flat and covered in grass or other vegetation. The image has been enhanced to show more detail.

RS-MoE: This image is a low-resolution aerial photograph of an airport. There are a lot of trees in the lower left corner of the image. There's an airport in the right of the image, with many planes and two large white buildings. There is a forest in the upper right of the image. There is an airport in the right of the image, to the right of the airport are two white buildings and to the right are some aeroplanes. On the left side of the airport is a forest and some grey buildings, and there are many roads through the airport.



RSGPT: The image is an aerial view of a river with several bridges crossing over it. There are several artificial islands in the middle of the river. The area around the river is mostly green grass and trees. There are some buildings visible in the distance. There are some ships on the river. The image is clear and detailed, showing the various structures and landscapes in the area.

RS-MoE: This is a satellite overlook of a river. In the centre of the image there is a man-made island that divides the river into two parts. There is a waterfall on the left side of the image. There are some trees on both sides of the river. There is a bridge that crosses the river over the island. There are some cars on the bridge. On the left of the island there is a waterfall.

Fig. 5. Qualitative results of image captions generated by RSGPT and our RS-MoE model for two randomly selected remote sensing images from the RSICD dataset. In captions generated by our model, different colors indicate distinct aspects of the image: orange for the overall theme, purple for objects within the scene, and green for spatial relationships between objects.

TABLE IV
RESULTS OF OUR MODEL AND STATE-OF-THE-ART MODELS ON THE RSICD DATASET FOR RSIC TASK.

Method	BLEU-1	BLEU-2	BLEU-3	BLEU-4	METEOR	ROUGE_L	CIDEr
VLAD + RNN [29]	49.38	30.91	22.09	16.77	19.96	42.42	103.92
VLAD + LSTM [29]	50.04	31.95	23.19	17.78	20.46	43.34	118.01
mRNN [30]	45.58	28.25	18.09	12.13	15.69	31.26	19.15
mLSTM [30]	50.57	32.42	23.29	17.46	17.84	35.02	31.61
mGRU [31]	42.56	29.99	22.91	17.98	19.41	37.97	124.82
mGRU embedword [31]	60.94	46.24	36.80	29.81	26.14	48.20	159.54
CSMLF [32]	57.59	38.59	28.32	22.17	21.28	44.55	52.97
SAA [33]	59.35	45.11	35.29	28.08	26.11	49.57	132.35
Soft-attention [34]	65.13	49.04	39.00	32.30	26.39	49.69	90.58
SD-RSIC [35]	64.50	47.10	36.40	29.40	24.90	51.90	77.50
RTRMN (semantic) [36]	62.01	46.23	36.44	29.71	28.29	55.39	151.46
RTRMN (statistical) [36]	61.02	45.14	35.35	28.59	27.51	54.52	148.20
SVM-D BOW [37]	61.12	42.77	31.53	24.11	23.03	45.88	68.25
SVM-D CONC [37]	59.99	43.47	33.55	26.89	22.99	45.57	68.54
MLAT [42]	66.90	51.13	41.14	34.21	27.31	50.57	94.27
Post-processing [38]	62.90	45.99	35.68	28.68	25.30	47.34	75.56
RSGPT-13B [15]	70.32	54.23	44.02	36.83	30.10	53.34	102.94
RS-CapRet-7B [41]	72.00	59.90	50.60	43.30	37.00	63.30	250.20
RS-MoE-7B w/o finetuning	78.61	63.60	51.44	43.35	39.30	60.77	109.46

its ability to perform well across diverse datasets without requiring dataset-specific adjustments.

To further illustrate the effectiveness of the generated captions, we selected two remote sensing images from the test set of the RSICD dataset and displayed the captioning

results generated by RSGPT and our model in Figure 5. It is evident from Figure 5 that, unlike RSGPT, our RS-MoE model accurately describes the spatial positions of objects within the images. This capability demonstrates RS-MoE's enhanced ability to capture and articulate spatial relationships

TABLE V
COMPARISON RESULTS OF DIFFERENT NUMBERS OF LLMs IN THE MOE BLOCK ON THE RSICAP DATASET FOR THE RSIC TASK.

Number of LLMs	BLEU-1	BLEU-2	BLEU-3	BLEU-4	METEOR	ROUGE_L	CIDEr
1	48.51	38.65	29.57	25.13	23.01	21.49	93.51
2	64.52	51.32	40.43	33.42	30.61	28.27	124.41
3	82.13	65.44	51.93	42.55	40.28	35.72	158.36
4	77.36	60.38	48.91	39.26	37.94	32.95	147.24

TABLE VI
COMPARISON RESULTS OF DIFFERENT LLM MODEL IN THE MOE BLOCK ON THE RSICAP DATASET FOR THE RSIC TASK.

LLM in MoE Block	BLEU-1	BLEU-2	BLEU-3	BLEU-4	METEOR	ROUGE_L	CIDEr
Llama-3.2-1B [27]	57.36	42.25	22.14	20.54	32.36	25.98	109.37
StableLM-1.6B [43]	56.42	44.36	23.27	22.14	33.71	24.62	110.85
Qwen-1.8B [44]	59.35	47.28	27.52	22.95	34.62	25.38	113.98
Phi2-2.7B [45]	59.78	48.15	27.35	25.58	36.77	25.36	114.96
Llama-3.2-3B [27]	65.11	52.44	28.78	26.86	40.04	27.62	120.20
LLaMa-7B [46]	77.95	62.11	49.28	40.27	38.26	31.91	150.31
Vicuna-7B[28]	82.13	65.44	51.93	42.55	40.28	35.72	158.36

and arrangements, which are essential for a comprehensive understanding of remote sensing imagery. By providing detailed, contextually rich descriptions that reflect the actual scene, RS-MoE ensures that the generated captions are both informative and precise, thereby improving the overall interpretability of remote sensing data.

V. DISCUSSION

In this section, we conduct a comprehensive analysis of the effectiveness and generalizability of the proposed RS-MoE model from two perspectives. Firstly, we verify the effectiveness of our model and training strategy through three specific ablation studies. Specifically, the first ablation study investigates the impact of varying the number of LLMs within the MoE block. The second study assesses the effects of using different types of LLMs on model performance. The third ablation study focuses on evaluating the effectiveness of our two-stage training strategy. Subsequently, we extend the application of our model to the Remote Sensing Visual Question Answering (RSVQA) task to assess its broader applicability and generalization capabilities across diverse contexts.

A. Ablation Study

1) *Effect of Different Numbers of LLMs in the MoE Block:* As described in Section III-B, within the MoE-Block, we employ an instruction router to generate three detailed prompts, each directed to a distinct Large Language Model (LLM) to independently handle the overall theme, geographic objects, and relationships among objects in remote sensing images. In this section, we analyze the results obtained from using varying numbers of LLMs. Specifically, we trained versions of the RS-MoE model with one to four LLMs on the RSICap

dataset, keeping the first stage constant while adjusting the number of LLMs in the second stage. When the number of LLMs is set to 1, the model reduces to a conventional single-LLM decoder VLM. With two LLMs, each LLM is tasked with describing either the image's theme or specific information. For configurations with four LLMs, we assign one LLM each to address the image's theme, objects, absolute positions of objects, and relationships among objects.

We evaluated the performance of these models on the RSIC task using the RSIEval dataset, with detailed results presented in Table V. By comparing the results for configurations with more than one LLM to those with only a single LLM, we observe substantial performance improvements when the task is divided into subtasks. This results further validates the effectiveness of incorporating the idea of MoE into the remote sensing image captioning task. Additionally, comparing the results for models with 2, 3, and 4 LLMs, we found that using three LLMs yields the best performance. Consequently, in our experiments, we employ three LLMs to focus on generating captions for the image's theme, included objects, and spatial relationships among objects, highlighting the advantage of the MoE framework for handling complex, multi-faceted tasks in remote sensing. This setup not only enhances the interpretability of the generated captions but also demonstrates the flexibility and scalability of our model when addressing intricate details in remote sensing imagery.

2) *Effect of Different LLM Models:* In this section, we investigate the effect of different lightweight LLMs within the MoE Block on remote sensing image captioning. Specifically, in addition to the original selection of Llama-3.2-1B, Llama-3.2-3B, and Vicuna-7B, we further experimented with four additional state-of-the-art LLMs from the computer vision

TABLE VII
COMPARISON RESULTS OF DIFFERENT TRAINING STRATEGY FOR OUR MODEL ON THE RSICAP DATASET FOR THE RSIC TASK.

Training Strategy	BLEU-1	BLEU-2	BLEU-3	BLEU-4	METEOR	ROUGE_L	CIDEr
One-Stage	50.39	33.44	24.37	20.86	27.49	25.36	98.21
Two-Stage	82.13	65.44	51.93	42.55	40.28	35.72	158.36

TABLE VIII
RESULTS OF OUR MODEL AND STATE-OF-THE-ART MODELS ON THE RSVQA TEST SET OF RSIEVAL.

Method	Presence	Quantity	Color	Absolute pos.	Relative pos.	Area comp.	Road dir.	Image	Scene	Reasoning	Avg accuracy
BLIP2	60.41	26.02	43.24	7.69	13.16	58.14	33.33	74.42	43.24	47.50	45.56
MiniGPT4	29.70	9.76	31.53	1.54	1.32	16.28	0.00	34.88	24.32	17.50	21.82
InstructBLIP	76.14	21.95	45.05	12.31	10.53	69.77	0.00	81.40	45.95	57.50	53.26
RSGPT	81.22	39.02	54.05	38.46	35.53	62.79	66.67	93.02	89.19	70.00	65.24
RS-MoE	83.16	32.77	71.92	43.95	45.00	63.41	0.00	77.89	93.18	74.07	68.65

field: Qwen-1.8B [44], StableLM-1.6B [43], Phi2-2.7B [45], and LLama-7B [46]. These models are designed to understand and generate human-like text across a wide range of topics, and we selected them to assess how different LLM configurations influence performance within our proposed RS-MoE.

Each of the seven RS-MoE model variants was trained as a baseline on the RSICap dataset and evaluated on the RSIEval dataset. The performance metrics are displayed in Table VI. As observed from the results, all selected lightweight LLMs under our MoE framework achieved reasonably satisfactory performance in remote sensing image captioning. This consistency across different LLMs demonstrates the robustness and adaptability of our proposed framework, indicating that even with various lightweight LLM configurations, the RS-MoE model is able to maintain effective and contextually relevant caption generation for complex remote sensing imagery. This suggests that the our MoE framework can be flexibly integrated with different LLMs, providing a versatile solution adaptable to the needs of various tasks and computational environments.

3) *Effect of Two-stage Training Strategy:* We further evaluate the effectiveness of our proposed two-stage training strategy. As explained in Section III-C, directly training our RS-MoE model can lead to performance degradation due to sparsity issues stemming from the distinct characteristics of remote sensing images compared to natural images. To validate this hypothesis, we implemented a baseline model trained using a single-stage approach, directly optimizing the model without employing the two-stage strategy. Comparative results for both training methods are shown in Table VII. The findings indicate that the two-stage training strategy significantly outperforms the single-stage approach, underscoring the advantages of this method. By incorporating the first training stage, the VLM encoder and LLM Block learn feature representations tailored to remote sensing imagery, gaining a foundational understanding of remote sensing-specific visual patterns and linguistic cues. This process establishes a robust basis for accurate feature extraction and preliminary captioning. This stage essentially fine-tunes the model's ability to interpret complex spatial arrangements and thematic elements unique to remote sensing imagery, elements often underrepresented in models pretrained

on natural images. In the second stage, the model builds upon this solid foundation, requiring only minimal fine-tuning to adapt the MoE block. Consequently, each LLM in the MoE block can effectively focus on its designated task, whether it involves capturing thematic elements, identifying specific geographic objects, or interpreting spatial relationships among objects. This task-oriented fine-tuning results in captions that are not only precise but also provide a comprehensive view of the remote sensing scene, with detailed and contextually relevant descriptions. Overall, this two-stage training strategy represents a core innovation of our work, demonstrating how carefully designed training frameworks can achieve superior results in the specialized domain of remote sensing.

B. Extension on the RSVQA Task

To verify the generalization of the proposed model, we further evaluated its performance on the visual question answering (VQA) task for remote sensing images. Specifically, we used the RSIEval dataset's 10 categories of questions, including presence, quantity, color, absolute position, relative position, area comparison, road direction, image, scene, and reasoning. We queried BLIP2, MiniGPT4, InstructBLIP, RSGPT, and our RS-MoE model, all of which were trained on the RSICap dataset, and calculated the average accuracy of their answers for each category. As shown in Table VIII, our model achieved the highest performance in seven out of the ten categories. To visually demonstrate the results on RSVQA, we randomly selected a remote sensing image from the dataset and displayed the answers provided by these models in four aspects: Theme, Quantity, Absolute Position, and Relative Position. It was observed that for simple Theme questions, all models were able to answer accurately. However, as the complexity of the questions increased, especially for those related to spatial relationships, the baseline models' performance deteriorated, while our model continued to provide accurate answers. This indicates that our model excels in handling complex questions, demonstrating its superior capability in understanding and reasoning about spatial relationships in remote sensing images.



Question: What is the theme of the image? (*Theme*)

Ground truth: Airport.

BLIP2:	This is an image of airplanes.	X
InstructBLIP:	An airport.	✓
MiniGPT4:	The theme of the image is an airport.	✓
RSGPT:	The theme of the image is an airport.	✓
RS-MoE:	The theme of the image is an airport.	✓

Question: How many airplanes are there in this image? (*Quantity*)

Ground truth: Three.

BLIP2:	There are two airplanes in this image.	X
InstructBLIP:	There are three airplanes in this image.	✓
MiniGPT4:	There are two airplanes parked at the gate in this image.	X
RSGPT:	There are two airplanes in this image.	X
RS-MoE:	There is an airport in the image with three airplanes in it.	✓

Question: Where is the terminal located in the image? (*Absolute Position*)

Ground truth: Lower left corner.

BLIP2:	There is a terminal in the image.	X
InstructBLIP:	The terminal is in the upper right corner of the image.	X
MiniGPT4:	The terminal located in the left of the image.	X
RSGPT:	The terminal is in the lower part of the image.	X
RS-MoE:	There is a terminal in the lower left corner of the image.	✓

Question: What is the relative position between the terminal and the airplanes? (*Relative Position*)

Ground truth: Surrounding the terminal.

BLIP2:	The airplanes is located in the lower left corner.	X
InstructBLIP:	The terminal is closer to the airplanes than they are to each other.	X
MiniGPT4:	The relative position between the terminal and the airplanes is that the airplanes are parked on the tarmac in front of the terminal building.	✓
RSGPT:	The airplanes is above the terminal.	X
RS-MoE:	There are some airplanes surrounding the terminal.	✓

Fig. 6. Qualitative results of visual question answering for remote sensing images by BLIP2, MiniGPT4, InstructBLIP, RSGPT, and our RS-MoE model on the RSVQA test set from the RSEval dataset.

VI. CONCLUSION

This paper introduces RS-MoE, a pioneering Mixture of Experts (MoE)-based Vision-Language Model (VLM) specifically developed for remote sensing image captioning. RS-MoE consists of three core modules: the Image Encoder, VLM Encoder, and MoE Block. At the heart of the framework, the MoE Block leverages an Instruction Router to dynamically generate task-specific prompts, guiding each Large Language Model (LLM) in subsequent layers to focus on distinct aspects of captioning—theme comprehension, object identi-

fication, and relationship interpretation. This design allows the model to capture intricate semantic features unique to remote sensing imagery, enabling the generation of detailed, contextually accurate captions. Additionally, we propose a two-stage training strategy to address performance degradation from sparsity issues inherent in MoE-based methods and enhance training efficiency. Our extensive experiments show that, even after fine-tuning on only one dataset, RS-MoE achieves state-of-the-art performance across four RSIC datasets and demonstrates robust generalization capabilities on an RSVQA

dataset. Notably, our lightweight RS-MoE-1B variant achieves performance comparable to larger 13B VLMs, underscoring the model's efficiency in remote sensing applications. Thus, RS-MoE not only excels in performance but also proves practical for real-world applications, particularly in resource-constrained environments where computational efficiency is essential.

REFERENCES

- [1] Z. Shi and Z. Zou, "Can a machine generate humanlike language descriptions for a remote sensing image?" *IEEE Transactions on Geoscience and Remote Sensing*, vol. 55, no. 6, pp. 3623–3634, 2017.
- [2] Y. Gong, L. Wang, M. Hodosh, J. Hockenmaier, and S. Lazebnik, "Improving image-sentence embeddings using large weakly annotated photo collections," in *Computer Vision–ECCV 2014: 13th European Conference, Zurich, Switzerland, September 6–12, 2014, Proceedings, Part IV 13*. Springer, 2014, pp. 529–545.
- [3] C. Sun, C. Gan, and R. Nevatia, "Automatic concept discovery from parallel text and visual corpora," in *Proceedings of the IEEE international conference on computer vision*, 2015, pp. 2596–2604.
- [4] X. Shen, B. Liu, Y. Zhou, J. Zhao, and M. Liu, "Remote sensing image captioning via variational autoencoder and reinforcement learning," *Knowledge-Based Systems*, vol. 203, p. 105920, 2020.
- [5] R. Zhao, Z. Shi, and Z. Zou, "High-resolution remote sensing image captioning based on structured attention," *IEEE Transactions on Geoscience and Remote Sensing*, vol. 60, pp. 1–14, 2021.
- [6] U. Zia, M. M. Riaz, and A. Ghafoor, "Transforming remote sensing images to textual descriptions," *International Journal of Applied Earth Observation and Geoinformation*, vol. 108, p. 102741, 2022.
- [7] T. Wei, W. Yuan, J. Luo, W. Zhang, and L. Lu, "Vlca: vision-language aligning model with cross-modal attention for bilingual remote sensing image captioning," *Journal of Systems Engineering and Electronics*, vol. 34, no. 1, pp. 9–18, 2023.
- [8] A. Radford, J. W. Kim, C. Hallacy, A. Ramesh, G. Goh, S. Agarwal, G. Sastry, A. Askell, P. Mishkin, J. Clark *et al.*, "Learning transferable visual models from natural language supervision," in *International conference on machine learning*. PMLR, 2021, pp. 8748–8763.
- [9] K. Zhou, J. Yang, C. C. Loy, and Z. Liu, "Learning to prompt for vision-language models," *International Journal of Computer Vision*, vol. 130, no. 9, pp. 2337–2348, 2022.
- [10] C. Wen, J. Liang, S. Yuan, H. Huang, and Y. Fang, "How secure are large language models (llms) for navigation in urban environments?" *arXiv preprint arXiv:2402.09546*, 2024.
- [11] J. Li, D. Li, S. Savarese, and S. Hoi, "Blip-2: Bootstrapping language-image pre-training with frozen image encoders and large language models," in *International conference on machine learning*. PMLR, 2023, pp. 19730–19742.
- [12] D. Zhu, J. Chen, X. Shen, X. Li, and M. Elhoseiny, "Minigpt-4: Enhancing vision-language understanding with advanced large language models," *arXiv preprint arXiv:2304.10592*, 2023.
- [13] W. Dai, J. Li, D. Li, A. M. H. Tiong, J. Zhao, W. Wang, B. Li, P. Fung, and S. Hoi, "Instructblip: Towards general-purpose vision-language models with instruction tuning," *arXiv preprint arXiv:2305.06500*, 2023.
- [14] X. Li, C. Wen, Y. Hu, and N. Zhou, "Rs-clip: Zero shot remote sensing scene classification via contrastive vision-language supervision," *International Journal of Applied Earth Observation and Geoinformation*, vol. 124, p. 103497, 2023.
- [15] Y. Hu, J. Yuan, C. Wen, X. Lu, and X. Li, "Rsrgpt: A remote sensing vision language model and benchmark," *arXiv preprint arXiv:2307.15266*, 2023.
- [16] K. Kuckreja, M. S. Danish, M. Naseer, A. Das, S. Khan, and F. S. Khan, "Geochat: Grounded large vision-language model for remote sensing," 2023.
- [17] C. Pang, J. Wu, J. Li, Y. Liu, J. Sun, W. Li, X. Weng, S. Wang, L. Feng, G.-S. Xia, and C. He, "H2rsvlm: Towards helpful and honest remote sensing large vision language model," 2024.
- [18] W. Zhang, M. Cai, T. Zhang, Y. Zhuang, and X. Mao, "Earthgpt: A universal multi-modal large language model for multi-sensor image comprehension in remote sensing domain," *arXiv preprint arXiv:2401.16822*, 2024.
- [19] D. Hong, B. Zhang, X. Li, Y. Li, C. Li, J. Yao, N. Yokoya, H. Li, P. Ghamisi, X. Jia, A. Plaza, P. Gamba, J. A. Benediktsson, and J. Chanussot, "Spectralgpt: Spectral remote sensing foundation model," *IEEE Transactions on Pattern Analysis and Machine Intelligence*, vol. 46, no. 8, pp. 5227–5244, 2024, doi:10.1109/TPAMI.2024.3362475.
- [20] D. Hong, C. Li, B. Zhang, N. Yokoya, J. A. Benediktsson, and J. Chanussot, "Multimodal artificial intelligence foundation models: Unleashing the power of remote sensing big data in earth observation," *The Innovation Geoscience*, vol. 2, no. 1, pp. 100055–1, 2024.
- [21] H. Liu, C. Li, Q. Wu, and Y. J. Lee, "Visual instruction tuning," *Advances in neural information processing systems*, vol. 36, 2024.
- [22] P. Wang, S. Bai, S. Tan, S. Wang, Z. Fan, J. Bai, K. Chen, X. Liu, J. Wang, W. Ge *et al.*, "Qwen2-vl: Enhancing vision-language model's perception of the world at any resolution," *arXiv preprint arXiv:2409.12191*, 2024.
- [23] C. Wen, Y. Hu, X. Li, Z. Yuan, and X. X. Zhu, "Vision-language models in remote sensing: Current progress and future trends," *arXiv preprint arXiv:2305.05726*, 2023.
- [24] X. Zhai, A. Kolesnikov, N. Houlsby, and L. Beyer, "Scaling vision transformers," in *Proceedings of the IEEE/CVF conference on computer vision and pattern recognition*, 2022, pp. 12104–12113.
- [25] A. Yang, B. Yang, B. Hui, B. Zheng, B. Yu, C. Zhou, C. Li, C. Li, D. Liu, F. Huang *et al.*, "Qwen2 technical report," *arXiv preprint arXiv:2407.10671*, 2024.
- [26] F. Li, R. Zhang, H. Zhang, Y. Zhang, B. Li, W. Li, Z. Ma, and C. Li, "Llava-next-interleave: Tackling multi-image, video, and 3d in large multimodal models," *arXiv preprint arXiv:2407.07895*, 2024.
- [27] A. Dubey, A. Jauhri, A. Pandey, A. Kadian, A. Al-Dahle, A. Letman, A. Mathur, A. Schelten, A. Yang, A. Fan *et al.*, "The llama 3 herd of models," *arXiv preprint arXiv:2407.21783*, 2024.
- [28] W.-L. Chiang, Z. Li, Z. Lin, Y. Sheng, Z. Wu, H. Zhang, L. Zheng, S. Zhuang, Y. Zhuang, J. E. Gonzalez, I. Stoica, and E. P. Xing, "Vicuna: An open-source chatbot impressing gpt-4 with 90%* chatgpt quality," March 2023. [Online]. Available: <https://lmsys.org/blog/2023-03-30-vicuna/>
- [29] X. Lu, B. Wang, X. Zheng, and X. Li, "Exploring models and data for remote sensing image caption generation," *IEEE Transactions on Geoscience and Remote Sensing*, vol. 56, no. 4, pp. 2183–2195, 2017.
- [30] B. Qu, X. Li, D. Tao, and X. Lu, "Deep semantic understanding of high resolution remote sensing image," in *2016 International conference on computer, information and telecommunication systems (Cits)*. IEEE, 2016, pp. 1–5.
- [31] X. Li, A. Yuan, and X. Lu, "Multi-modal gated recurrent units for image description," *Multimedia Tools and Applications*, vol. 77, pp. 29847–29869, 2018.
- [32] B. Wang, X. Lu, X. Zheng, and X. Li, "Semantic descriptions of high-resolution remote sensing images," *IEEE Geoscience and Remote Sensing Letters*, vol. 16, no. 8, pp. 1274–1278, 2019.
- [33] X. Lu, B. Wang, and X. Zheng, "Sound active attention framework for remote sensing image captioning," *IEEE Transactions on Geoscience and Remote Sensing*, vol. 58, no. 3, pp. 1985–2000, 2019.
- [34] K. Xu, J. Ba, R. Kiros, K. Cho, A. Courville, R. Salakhudinov, R. Zemel, and Y. Bengio, "Show, attend and tell: Neural image caption generation with visual attention," in *International conference on machine learning*. PMLR, 2015, pp. 2048–2057.
- [35] G. Sumbul, S. Nayak, and B. Demir, "Sd-rsic: Summarization-driven deep remote sensing image captioning," *IEEE Transactions on Geoscience and Remote Sensing*, vol. 59, no. 8, pp. 6922–6934, 2020.
- [36] B. Wang, X. Zheng, B. Qu, and X. Lu, "Retrieval topic recurrent memory network for remote sensing image captioning," *IEEE Journal of Selected Topics in Applied Earth Observations and Remote Sensing*, vol. 13, pp. 256–270, 2020.
- [37] G. Hoxha and F. Melgani, "A novel svm-based decoder for remote sensing image captioning," *IEEE Transactions on Geoscience and Remote Sensing*, vol. 60, pp. 1–14, 2021.
- [38] G. Hoxha, G. Scuccato, and F. Melgani, "Improving image captioning systems with post-processing strategies," *IEEE Transactions on Geoscience and Remote Sensing*, 2023.
- [39] Y. Zhan, Z. Xiong, and Y. Yuan, "Skyeyegept: Unifying remote sensing vision-language tasks via instruction tuning with large language model," *arXiv preprint arXiv:2401.09712*, 2024.
- [40] Y. Bazi, L. Bashmal, M. M. Al Rahhal, R. Ricci, and F. Melgani, "Rs-llava: A large vision-language model for joint captioning and question answering in remote sensing imagery," *Remote Sensing*, vol. 16, no. 9, p. 1477, 2024.

[41] J. D. Silva, J. Magalhães, D. Tuia, and B. Martins, “Large language models for captioning and retrieving remote sensing images,” *arXiv preprint arXiv:2402.06475*, 2024.

[42] C. Liu, R. Zhao, and Z. Shi, “Remote-sensing image captioning based on multilayer aggregated transformer,” *IEEE Geoscience and Remote Sensing Letters*, vol. 19, pp. 1–5, 2022.

[43] M. Bellagente, J. Tow, D. Mahan, D. Phung, M. Zhuravinskyi, R. Adithyan, J. Baicoianu, B. Brooks, N. Cooper, A. Datta *et al.*, “Stable lm 2 1.6 b technical report,” *arXiv preprint arXiv:2402.17834*, 2024.

[44] J. Bai, S. Bai, Y. Chu, Z. Cui, K. Dang, X. Deng, Y. Fan, W. Ge, Y. Han, F. Huang *et al.*, “Qwen technical report,” *arXiv preprint arXiv:2309.16609*, 2023.

[45] M. Javaheripi, S. Bubeck, M. Abdin, J. Aneja, S. Bubeck, C. C. T. Mendes, W. Chen, A. Del Giorno, R. Eldan, S. Gopi *et al.*, “Phi-2: The surprising power of small language models,” *Microsoft Research Blog*, 2023.

[46] H. Touvron, T. Lavril, G. Izacard, X. Martinet, M.-A. Lachaux, T. Lacroix, B. Rozière, N. Goyal, E. Hambro, F. Azhar *et al.*, “Llama: Open and efficient foundation language models,” *arXiv preprint arXiv:2302.13971*, 2023.



Hui Lin received the Bachelor’s degree in Space Information and Digital Technology from Wuhan University, Wuhan, China, in 2012, and the Ph.D. degree in Cartography and Geographic Information Systems from the Institute of Remote Sensing and Digital Earth, Chinese Academy of Sciences, in 2017. He is currently a Senior Engineer in China Academy of Electronics and Information Technology, Beijing, China. His research interests include multimodal data fusion, deep learning, and remote sensing applications.



Danfeng Hong (Senior Member, IEEE) received the Dr.-Ing. degree (summa cum laude) from the Signal Processing in Earth Observation (SiPEO), Technical University of Munich (TUM), Munich, Germany, in 2019.

Since 2022, he has been a Full Professor with the Aerospace Information Research Institute, Chinese Academy of Sciences, Beijing, China. His research interests include artificial intelligence, multimodal remote sensing, foundation models, hyperspectral imaging, and Earth observation.

Dr. Hong is an Associate Editor for the IEEE TRANSACTIONS ON GEOSCIENCE AND REMOTE SENSING (TGRS) and the IEEE TRANSACTIONS ON IMAGE PROCESSING (TIP), and the Editorial Board Member of *Information Fusion*, *ISPRS Journal of Photogrammetry and Remote Sensing*, and *International Journal of Applied Earth Observation and Geoinformation*. He received the Jose Bioucas Dias Award for recognizing an outstanding paper at WHISPERS in 2021, the Remote Sensing Young Investigator Award in 2022, the IEEE GRSS Early Career Award in 2022, the MIT Technology Review & DeepTech “China’s Intelligent Computing Innovators” award in 2024, and a Highly Cited Researcher (Clarivate Analytics/Thomson Reuters) since 2022.



Shuhang Ge received his B.S. degree in Century College, Beijing University of Posts and Telecommunications in 2022, and his master degree from New York University in 2024. He is currently a Machine Learning Engineer at ByteDance. His research interests include Large Language Models, Multimodal Artificial Intelligence and Generation Models.



Chuyao Luo is currently a Associate Researcher at Harbin Institute of Technology (Shenzhen). He received his Bachelor’s degree in Internet of things Engineering from Dalian Maritime University. He received his Doctor’s degree in Computer Science at Harbin Institute of Technology (Shenzhen). His research includes data mining, computer vision, time-series data prediction, and precipitation nowcasting.



Kai Jiang received Ph.D. degree from the University of Science and Technology of China, Anhui, China, in 2014. Kai Jiang is a Senior Engineer in Nanjing Research Institute of Electronic Engineering. He is the head of Key Lab of Information System Requirement. His main research interests are systems engineering, data mining, and large scale system architecture.



Hao Jin received Ph.D. degree from Institute of Information Engineering, Chinese Academy of Sciences, Beijing, China, in 2018. Hao Jin is a Senior Engineer in National Engineering Research Center for Public Safety Risk Perception and Control by Big Data (RPP), China Academic of Electronics and Information Technology. Her main research interests are artificial intelligence and big data.



Congcong Wen (Member, IEEE) received his B.S. degree in Geographic Information Systems from the China University of Petroleum, China, in 2016, and his Ph.D. degree from the Aerospace Information Research Institute, Chinese Academy of Sciences, China, in 2021. He is currently a Postdoctoral Associate with the Department of Electrical and Computer Engineering at New York University and New York University Abu Dhabi. His research interests include multimodal artificial intelligence, 3D computer vision, foundation models, and remote sensing.